Effect of Water Contact on the Density Distributions of Thin Supported Polymer Films Investigated by an X-ray Reflectivity Method

ARTICLE *in* LANGMUIR · NOVEMBER 2010

Impact Factor: 4.46 · DOI: 10.1021/la1035085 · Source: PubMed

4 AUTHORS, INCLUDING:

Jin Goo Yoon
Pohang University of Science and Technology
6 PUBLICATIONS **12** CITATIONS
SEE PROFILE

Jae Hyun Kim
Samsung
65 PUBLICATIONS **505** CITATIONS
SEE PROFILE

Langmuir
Article
pubs.acs.org/Langmuir

Effect of Water Contact on the Density Distributions of Thin Supported Polymer Films Investigated by an X-ray Reflectivity Method

Sung Il Ahn,[†] Jin Goo Yoon,[†] Jae Hyun Kim,[‡] and Wang-Cheol Zin*,[†]

[†]*Department of Materials Science and Engineering, POSTECH, Pohang-city, Gyeongbuk, South Korea, and* [‡]*Memory Division, Samsung Electronics Co. Ltd, Hwasung-city, Gyeonggi-do, South Korea*

Received September 2, 2010

The diffusion processes of water molecules into polymer films (PMMA/PS homopolymers and random copolymers) in contact with liquid water were investigated using gravimetric methods and X-ray reflectivity (XRR) analysis. Methods of water contact and XRR measurement were designed for studying the systems in the nonequilibrium state of diffusion. Gravimetric measurements confirmed the Fickian diffusion behavior of films in contact with water. Vertical density distributions in PMMA and methylmethacrylate-rich copolymer films demonstrate the existence of a water-rich layer at the interface. However, with further absorption of water into the film, the overall density increased throughout the film. The results suggest that the diffusion of water into the polymer film occurs to recover density uniformity with a high concentration of water molecules at the surface. Some XRR data for the PS- and styrene-rich copolymer films could not be fit and converted to a vertical density distribution because of their huge diffusion coefficients. However, the reflectivity curves for these films and the vertical density distribution after sufficient water contact suggested that the surfaces of these films were commonly diffused after water contact. Atomic force microscopy (AFM) analysis demonstrated that the surface roughness of these films actually increased with water content.

1. Introduction

The effect of direct water contact on thin supported polymer films is important in several industrial fields.[1−7] To facilitate applications of these polymer films, basic information is necessary, including the distribution of water inside thin films in contact with liquid water, morphological changes in the film surface induced by water contact, and changes in diffusion behavior inside thin polymer films after water contact. In particular, the diffusion processes and distribution of water inside ultrathin polymer films remain poorly understood because appropriate methods to analyze these systems are not available.

Water diffusion at equilibrium inside polymer films has typically been investigated for films in contact with water vapor (humid air).[8−12] By neutron reflectivity (NR) analysis, for example, Vogt et al. found that a relatively large number of water molecules accumulate near the interface region between a polymer film and an SiO_2 substrate in the equilibrium state of diffusion.[10] This interfacial accumulation may be due predominantly to the attractive force between the water molecules and the SiO_2 substrate. In this study, films were exposed directly to water rather than to water vapor, and a more detailed model of the density profile of the polymer thin film was introduced. From these changes, we expect to discover an extended stage of diffusion and to present a novel approach to understanding water diffusion processes inside thin polymer films.

Direct water contact can cause diffusion behaviors that differ from those associated with contact with water vapor, particularly in the equilibrium state of diffusion. In both cases, Fick's law of diffusion is usually suggested for diffusion behavior.[12,13] Theoretically, Fick's law shows that systems with liquid water and water vapor in contact with the surface differ only in the initial concentration of water on the surface. If the diffusion behavior at a higher initial concentration still follows Fick's law, then electron density changes after direct water contact will simply be faster than those of the film in contact with water vapor. However, in the equilibrium state of diffusion, further stages of diffusion or different types of diffusion behavior can be expected because of the high concentration of water molecules at the surface of the film. In fact, many former studies[14−18] also show that the physical properties of thin film are influenced more seriously by surface effect as the thickness of the film decreases.

*Corresponding author. Phone: +81-54-279-2136. E-mail: wczin@postech.ac.kr.

(1) Hinsberg, W.; Wallraff, G.; Larson, C.; Davis, B.; Deline, V.; Raoux, S.; Miller, D.; Houle, F.; Hoffnagle, J.; Sanchez, M.; Rettner, C.; Sundberg, L.; Medeiros, D.; Dammel, R.; Conley, W. *Proc. SPIE* **2004**, *5376*, 21.
(2) Mulkens, J.; Flagello, D.; Streefkerk, B.; Graeupner, P. *J. Microlithogr., Microfabr., Microsyst.* **2004**, *3*, 104–114.
(3) Switkes, M.; Rothschild, M.; Kunz, R. R.; Baek, S.-Y.; Cole, D.; Yeung, M. *Microlithogr. World* **2003**, 4.
(4) Korzhenko, A. A.; Tabellout, M.; Emery, J. R. *Mater. Chem. Phys.* **2000**, *65*, 253–260.
(5) Leng, A.; Streckel, H.; Hofmann, K.; Stratmann, M. *Corros. Sci.* **1999**, *41*, 599–620.
(6) Sakai, Y.; Sadaoka, Y.; Matsuguchi, M. *Sens. Actuators, B* **1996**, *35*, 85–90.
(7) Smith, A. L.; Mulligan, R. B., Sr.; Shirazi, H. M. *J. Polym. Sci., Part B: Polym. Phys.* **2004**, *42*, 3893–3906.
(8) McDonough, L. A.; Dragnea, B.; Preusser, J.; Leone, S. R.; Hinsberg, W. D. *J. Phys. Chem. B* **2003**, *107*, 4951–4954.
(9) Sinha, S. K.; Sirota, E. B.; Garoff, S. *Phys. Rev. B* **1988**, *38*, 2297.
(10) Vogt, B. D.; Soles, C. L.; Jones, R. L.; Wang, C. Y.; Lin, E. K.; Wu, W. L.; Satija, S. K.; Goldfarb, D. L.; Angelopoulos, M. *Langmuir* **2004**, *20*, 5285–5290.
(11) Vogt, B. D.; Soles, C. L.; Lee, H. J.; Lin, E. K.; Wu, W. *Polymer* **2005**, *46*, 1635–1642.
(12) Vogt, B. D.; Soles, C. L.; Lee, H. J.; Lin, E. K.; Wu, W. L. *Langmuir* **2004**, *20*, 1453–1458.
(13) Goodelle, J. P.; Pearson, R. A.; Santore, M. M. *J. Appl. Polym. Sci.* **2002**, *86*, 2463–2471.
(14) DeMaggio, G. B.; Frieze, W. E.; Gidley, D. W.; Zhu, M.; Hristov, H. A.; Yee, A. F. *Phys. Rev. Lett.* **1997**, *78*, 1524–1527.
(15) Forrest, J. A.; Dalnoki-Veress, K. *Adv. Colloid Interface Sci.* **2001**, *94*, 167–196.
(16) Forrest, J. A.; DalnokiVeress, K.; Stevens, J. R.; Dutcher, J. R. *Phys. Rev. Lett.* **1996**, *77*, 2002–2005.
(17) Grohens, Y.; Brogly, M.; Labbe, C.; David, M. O.; Schultz, J. *Langmuir* **1998**, *14*, 2929.
(18) Keddie, J. L.; Jones, R. A. L.; Cory, R. A. *Faraday Discuss.* **1994**, 219–230.

One possible problem with earlier research is that the vertical film density before humidity contact was assumed to be uniform in X-ray reflectivity (XRR) and neutron reflectivity (NR) analyses. However, some studies,[19−21] have reported that the film is not of uniform density. Advanced analysis techniques have revealed small density fluctuations inside polymer thin films.[9,19,20] The vertical density fluctuation is mainly caused by the chain conformation effect and by interactions between the film and the surrounding medium. An understanding of the diffusion in thin films can be changed by this awareness of small density fluctuations in polymer films.

XRR and NR methods are useful for investigating the diffusion of small molecules inside thin films because these methods can be used to obtain the changes in density distributions.[22−30] Several studies on the water distribution inside thin polymer films have been conducted using these methods.[12,31−33] In the case of neutron scattering, it is possible to obtain a high contrast with deuterium indexing as a result of the distinct scattering length density of deuterium compared to that of other atoms, whereas X-rays can detect only the contrast in electron density.[34] Therefore, NR with deuterated water (D_2O) is a more appropriate way to determine the water distribution inside polymer films than the X-ray method, especially if the electron density of the polymers is similar to that of water. However, NR usually requires a long time to obtain a result for a sample,[35] or the experiment can conducted only in facilities that can produce a high-flux neutron beam; therefore, usually only the equilibrium state of diffusion is examined. Lately, a high-flux X-ray beam generated by synchrotron radiation has enabled the observation of the diffusion mechanism at short measurement times without unacceptably reducing the signal-to-noise (S/N) ratio. Because the goal of this study was to monitor the middle stages of diffusion in the film as well as the equilibrium state, XRR was used instead of NR. In addition, to compensate for the deficiencies of XRR and to analyze even small changes in the electron density distribution, several methods that were established in our previous study[19] were used in this study.

2. Experiments

2.1. Materials. Poly(methylmethacrylate) (PMMA, Pressure Chemical, 93,300 g/mol), polystyrene (PS, Pressure Chemical, 90,000 g/mol), and three types of poly(styrene-*ran*-methylmethacrylate) (Polymer Source), including MRAN (12% styrene mol fraction, 128,300 g/mol), MAS (46% styrene mol fraction, 66,000 g/mol), and SRAN (84% styrene mol fraction, 88,500 g/mol) were prepared as solutions in toluene. Si wafers with native oxide were precisely cut into 25 × 25 mm^2 pieces, cleaned with piranha solution, and then rinsed with DI water and dried in a stream of nitrogen. Polymer solutions were filtered using 45 μm syringe filters and spin-coated (2000 rpm, 60 s) onto wafers. The resulting films were ∼20 nm thick. The spin-coated samples were thermally treated at 50 °C above their glass-transition temperature T_g for 24 h and then cooled to room temperature before the XRR measurements.

2.2. Gravimetric Measurement. For the gravimetric measurements, PMMA films with two thicknesses (67 and 157 nm) were spin-coated onto 4 in. Si wafers. After thermal treatment, a puddle of water was deposited on the film surface using a syringe. For each measurement, the puddle of water was carefully and completely removed using the syringe and cleaning paper under humid conditions, and the amount of uptake was quickly measured using a microbalance (Mettler Toledo, XS105, precision ∼0.01 mg). After measurement, the puddle of water was deposited again for the next measurement. At each measurement point, a bare Si substrate was also measured to control for instrumental fluctuations. Actual mass uptake was obtained by subtracting the fluctuation from the mass uptake to remove the error produced by the microbalance itself. Measurements were recorded for > 7 days.

2.3. X-ray Reflectivity Analysis. Specular XRR measurements were conducted using synchrotron radiation sources at X-ray diffraction beamline 10C1 of the Pohang Light Source in Pohang, South Korea. An X-ray beam (λ = 1.54 Å) was focused onto each sample using a collimating mirror. The angle of the incident beam is horizontal, so the detector was rotated by 2θ while the sample was rotated by θ during the measurements. A Huber six-circle goniometer was used to orient the specimens. The reflectivity was measured over the range of 0.1 to 5.2° of the angle of the detector (2θ). The measurement range was subdivided into 340 steps, and the detector counted X-rays for 1 s at each point (for a total of 6 min per set of measurements). Different numbers of aluminum attenuators were applied in subdivided ranges of the detecting angle to cover the narrow effective dynamic range (approximately 10^3) of the scintillation counter.[20]

Reflectivity curves were analyzed using a distorted wave Born approximation (DWBA)-based fitting algorithm,[20,36] which was used in our previous study.[19] The density profiles were obtained in terms of the scattering length density, which is linearly proportional to the electron density and can be regarded as the mass density among the same chemical structures.

2.4. Water Contact of Samples for XRR Analysis. XRR was first measured using a dry film, and then a puddle of water was formed on the film while maintaining the alignment of the goniometer system (Figure 1a). During water contact and XRR measurement after water contact, the sample stage was covered and sealed using a thin imide cap to preserve humidity. To minimize beam loss and unnecessary scattering, the imide film was very thin (< 10 μm).

(19) Ahn, S. I.; Kim, J.-H.; Kim, J. H.; Jung, J. C.; Chang, T.; Ree, M.; Zin, W.-C. *Langmuir* **2009**, *25*, 5667–5673.
(20) van der Lee, A.; Hamon, L.; Holl, Y.; Grohens, Y. *Langmuir* **2001**, *17*, 7664–7669.
(21) Bollinne, C.; Stone, V. W.; Carlier, V.; Jonas, A. M. *Macromolecules* **1999**, *32*, 4719.
(22) Ade, H.; Wang, C.; Garcia, A.; Yan, H.; Sohn, K. E.; Hexemer, A.; Bazan, G. C.; Nguyen, T.-Q.; Kramer, E. J. *J. Polym. Sci., Part B: Polym. Phys.* **2009**, *47*, 1291–1299.
(23) Harada, M.; Suzuki, T.; Ohya, M.; Kawaguchi, D.; Takano, A.; Matsushita, Y.; Torikai, N. *J. Polym. Sci., Part B: Polym. Phys.* **2009**, *43*, 1486–1494.
(24) Hamilton, W. A.; Smith, G. S.; Alcantar, N. A.; Majewski, J.; Toomey, R. G.; Kuhl, T. L. *J. Polym. Sci., Part B: Polym. Phys.* **2004**, *42*, 3290–3301.
(25) Smith, G. S.; Skidmore, C. B.; Howe, P. M.; Majewski, J. *J. Polym. Sci., Part B: Polym. Phys.* **2004**, *42*, 3258–3266.
(26) Granick, S.; Kumar, S. K.; Amis, E. J.; Antonietti, M.; Balazs, A. C.; Chakraborty, A. K.; Grest, G. S.; Hawker, C.; Janmey, P.; Kramer, E. J.; Nuzzo, R.; Russell, T. P.; Safinya, C. R. *J. Polym. Sci., Part B: Polym. Phys.* **2003**, *41*, 2755–2793.
(27) Lee, H.-J.; Soles, C. L.; Liu, D.-W.; Bauer, B. J.; Wu, W.-L. *J. Polym. Sci., Part B: Polym. Phys.* **2002**, *40*, 2170–2177.
(28) Parratt, L. G. *Phys. Rev.* **1954**, *95*, 359.
(29) Pedersen, J. S.; Hamley, I. W. *J. Appl. Crystallogr.* **1994**, *27*, 36.
(30) Tan, N. C. B.; Wu, W. L.; Wallace, W. E.; Davis, G. T. *J. Polym. Sci., Part B: Polym. Phys.* **1998**, *36*, 155–162.
(31) Kent, M. S.; McNamara, W. F.; Fein, D. B.; Domeier, L. A.; Wong, A. P. Y. *J. Adhes.* **1999**, *69*, 121–138.
(32) Kent, M. S.; Smith, G. S.; Baker, S. M.; Nyitray, A.; Browning, J.; Moore, G.; Hua, D. W. *J. Mater. Sci.* **1996**, *31*, 927–937.
(33) Wu, W. L.; Orts, W. J.; Majkrzak, C. J.; Hunston, D. L. *Polym. Eng. Sci.* **1995**, *35*, 1000–1004.
(34) Roe, R. J. *Methods of X-ray and Neutron Scattering in Polymer Science*; Oxford University Press: New York, 2000.
(35) Glidle, A.; Hillman, A. R.; Rydeo, K. S.; Smith, E. L.; Cooper, J.; Gadegaard, N.; Webster, J. R. P.; Dalgliesh, R.; Cubitt, R. *Langmuir* **2009**, *25*, 4093–4103.
(36) van der Lee, A.; Salah, F.; Harzallah, B. *J. Appl. Crystallogr.* **2007**, *40*, 820–833.

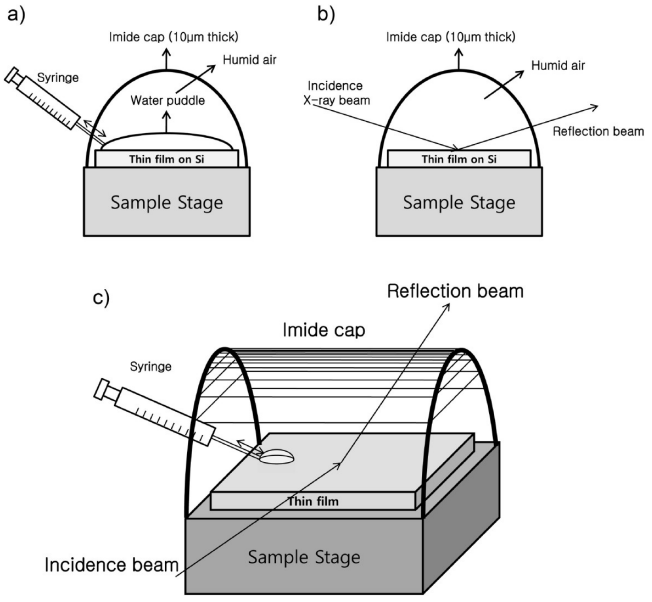

Figure 1. Schematic view of the water-contact method for XRR analysis. (a) The puddle of water was formed and removed using a syringe without contacting the polymer thin film. (b) Before XRR measurement, the puddle of water was removed and the sample was held in a small chamber under a thin imide cap filled with humid air to prevent the evaporation of water that had diffused into the film. (c) Elevated view of the system.

The puddle of water was removed carefully using a syringe right before the reflectivity was measured again (Figure 1c). Then the reflectivity was measured within 6 min (Figure 1b). In most cases, the puddle of water was successfully removed from the surface of the film. Although a very small droplet remained near the end of the needle, it did not affect the measurement because the beam passed far from it (> 1 cm).

2.5. AFM Measurement. Height profiles of the surfaces of selected samples were measured using an atomic force microscope (AFM) (Multimode, Digital Instruments) before and after water contact using the same methods of water supply and recovery as in the XRR measurements. The imide cap was not used in this system because air humidity can affect the measurement. To confirm any changes in the film due to the exposure to dry air during measurement, height profiles of the film after water contact were scanned repeatedly.

3. Results and Discussion

3.1. Gravimetric Measurements. The appropriate water-contact time for each sample was determined using the gravimetric method. Because the polymer thin films in this study were too thin (~20 nm) to determine mass changes using our microbalance, thick films (67 nm, 157 nm) were prepared that had weights that were large enough to measure. From the results obtained using thick films, the diffusion coefficient of water molecules inside the film was obtained so that the proper water-contact time of the thin film could be determined.

During the initial stage of diffusion, the normalized mass of water uptake was linearly related to the square root of the diffusion time (Figure 2). Because the water uptake in PMMA is known to follow Fick's law,[13,37] the linear region can be explained using a simplified form of Fick's law (eq 1) during

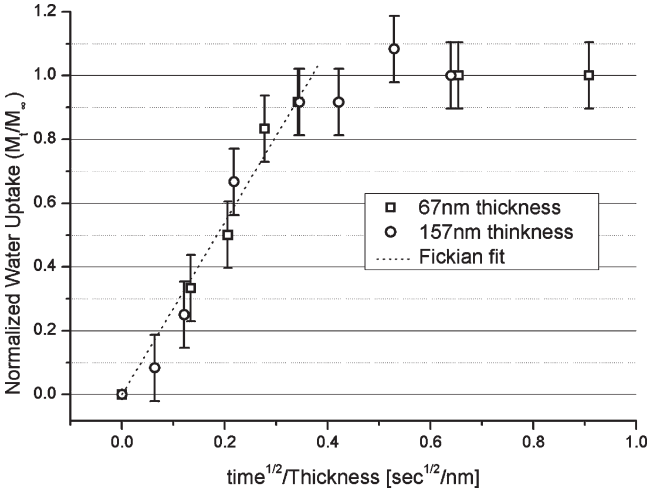

Figure 2. Water uptake results of PMMA films in the preliminary experiment. The thickness was measured by ellipsometry, and the error bars were determined on the basis of the microbalance manufacturer's data sheet. The dotted line indicates the early stage of the Fickian fit (eq 1).

Table 1. Water Contact Times (min) for Each Sample Chosen on the Basis of Preliminary Experiments

PMMA	MRAN	MAS	SRAN	PS
8	4	2	1.5	1
60	30	15	10	5
90	45	24	15	10
150	75	37	25	17
360	190	90	60	30

the initial stage of diffusion[38]

$$\frac{M_t}{M_\infty} = \frac{2}{l}\sqrt{\frac{Dt}{\pi}} \quad (1)$$

where M_t and M_∞ are the amount of water uptake at a certain time t and the saturation point respectively, l is the thickness of the film, and D is the diffusion coefficient of the film.

On the basis of the results (Figure 2) and Fick's law (eq 1), five appropriate distinct regimes were determined for PMMA films: an early stage of diffusion (8 min, stage 1), two stages around the point where the linearity of diffusion is broken (60 and 90 min, stages 2 and 3), and two stages in the saturation region (150 and 360 min, stages 4 and 5). Contact times for the PS films were also chosen after several preliminary experiments and a comparison of their diffusion coefficients with that of PMMA. In case of the random copolymers, the Fox equation based on the mole fractions was used to estimate the diffusion coefficients and water contact times (Table 1).

After the gravimetric measurements for water uptake of the above film, the films were used to check the constancy against external humidity during XRR measurement. Two opposing factors affect the reflectivity measurement time in this study: the measurement time must be sufficient to achieve an acceptable S/N ratio of the X-ray detector but short enough for the electron density profiles in films to remain constant. In our experiments, the S/N ratio was confirmed to be adequate; however, the question remains as to whether the measurement time used (6 min) is short enough to guarantee the constancy of the films. To confirm this, the gravimetric method was repeated with PMMA films of thickness 157 nm. Because the films were placed in contact with water for > 7 days, the diffusion processes were assumed to be in equilibrium.

(37) Turner, D. T. *Polymer* **1987**, *28*, 293.
(38) Crank, J. *The Mathematics of Diffusion*; Clarendon Press: Oxford, England, 1975.

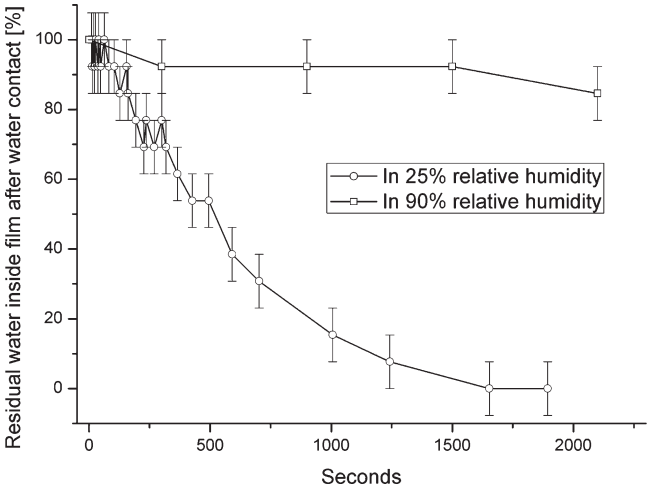

Figure 3. Evaporation percentages by mass for sufficiently wet PMMA films by water under different conditions. In dry air, all of the water in the film evaporated within 2000 s, but in humid air, the amount of water evaporated was less than the error range of the microbalance. The time for one set of X-ray reflectivity measurements was < 6 min.

Two of the wet films were placed in a humidity chamber ($> 90\%$ relative humidity at room temperature) and in a dry environment (25% relative humidity). Because the microbalance cannot be guaranteed to operate normally under humid conditions, the film in the humid chamber was measured on the microbalance under dry conditions and then quickly returned to the humidity chamber; the films were outside of the humidity chamber for < 10 s.

The evaporation of water out of the PMMA film was measured as a function of time, where the water content is expressed as a percentage of the water content achieved after placing the film in contact with water for > 7 days (Figure 3). Under dry conditions, all of the water in the film evaporated within 2000 s. In humid air, only a small quantity of water (within the range of the measurement error for the microbalance) was lost during 1500 s. Although this gravimetric result does not exclude the possibility of the diffusion of water molecules within the film, it does establish that the external flux of diffusion is negligible under humid conditions.

3.2. XRR Analysis. *3.2.1. Water Contact Effect on Reflectivity Curve.* Reflectivities were recorded for films of all compositions before and after water contact (Figure 4). Although the exact electron density distributions can be obtained only by the fitting process, some information such as the approximate thickness (where $t = 2\pi/\Delta q$ is the period of oscillation in the XRR curve) and diffusivity near the surface or interface (the amplitudes of oscillations) can be directly inferred from the geometric forms of the curves.

The amplitudes of the oscillations are regular within the measured range for the dry films, but for the wet films, the amplitudes decreased with increasing water contact time; in particular, the oscillations vanished as q_z increased in most systems. Such changes in oscillation amplitude typically occur as a result of increased interfacial roughness or instabilities in the uniformity of the density distributions in films.[9] Therefore, the results of the reflectivity measurements suggest that water contact induced serious changes in the density distributions within the films. These changes may be due to the diffusion of water molecules into the films and even to the deformation of the films; we will return to this issue in later sections in which we consider the density distributions.

The oscillations disappeared in the middle of the reflectivity curves for the wet MRAN film after 75 min of water contact (stage 4), for the MAS film after 37 min of water contact (stage 4), and for the SRAN film 25 min after water contact (stage 4). This disappearance of the oscillations is mainly due to the inhomogeneity of the vertical density inside film. The inhomogeneity of the density inside the film stimulates additional frequencies of oscillation in the XRR curve, and oscillations with different frequencies overlap so that destructive interference may occur. Therefore, it can be suggested that a density-rich layer may exist in the film at a certain time during water contact. Considering that diffusion stages 3 and 4 have different water contact times, these results are consistent with literature reports showing that water diffusion into a PMMA film is slower than that into a PS film.[39]

3.2.2. Failure of the Fitting Process for Some Samples. Vertical electron density distributions could not be obtained for stage 1 for MRAN, stages 1 and 2 for MAS, stages 1 and 2 for SRAN, and stages 1, 2, and 3 for PS. In those cases, the fitting program produced errors or physically unrealistic solutions, even though all possible mean densities (200 mean density values within $\pm 15\%$ of the bulk densities) were fitted. Significantly, the ability to fit the reflectivity curves was correlated to the water contact time and the mole fraction of styrene. One possible reason for this trend is the relatively large amount of deformation in the film density distribution during the reflectivity measurements. The measurement time was set to 6 min, which represents the optimum balance between achieving the lowest S/N ratio and the fastest detection time, but this time seems to have been too long to guarantee an invariant density distribution during the initial stages of diffusion in systems with fast diffusion of water into the film such as PS- and styrene-containing random copolymers. This suggestion is also supported by the fact that the density profiles of all films before water contact could be fitted normally.

3.3. Effects of Water Contact on Film Density Distributions. Some notable distributions of the scattering length density distribution listed in Table 2 are shown in Figures 5−7. On the basis of aspects of change in the film density distribution after water contact, the films can be divided into two groups: one consisting of PMMA and MRAN and the other consisting of MAS, SRAN, and PS. In both PMMA (Figure 5b) and MRAN films (Figure 6a), density-rich layers occurred after earlier stages that showed only weak changes in the density distribution. MAS, SRAN, and PS had similar diffusion tendencies (Figure 7) and similar electron density profiles before water contact.

In PMMA and MRAN, the overall electron densities of the low-density regions near the interfaces increased after the stages with density-rich layers. The density differences at each point on a density profile before and after water contact cannot be directly related to the existence of water because of the thickness differences induced by water contact. However, qualitative information on the diffusion process can be inferred from the geometrical changes in the shapes of the electron density profiles. In brief, water molecules that diffuse into the film first accumulate near the film−substrate interface and then in the rest of the film. One report[10] detected that water vapor accumulates near the interface between the polymer and the silicon oxide substrate; the authors suggested

(39) Linossier, I.; Gaillard, F.; Romand, M.; Feller, J. F. *J. Appl. Polym. Sci.* **1997**, *66*, 2465–2473.

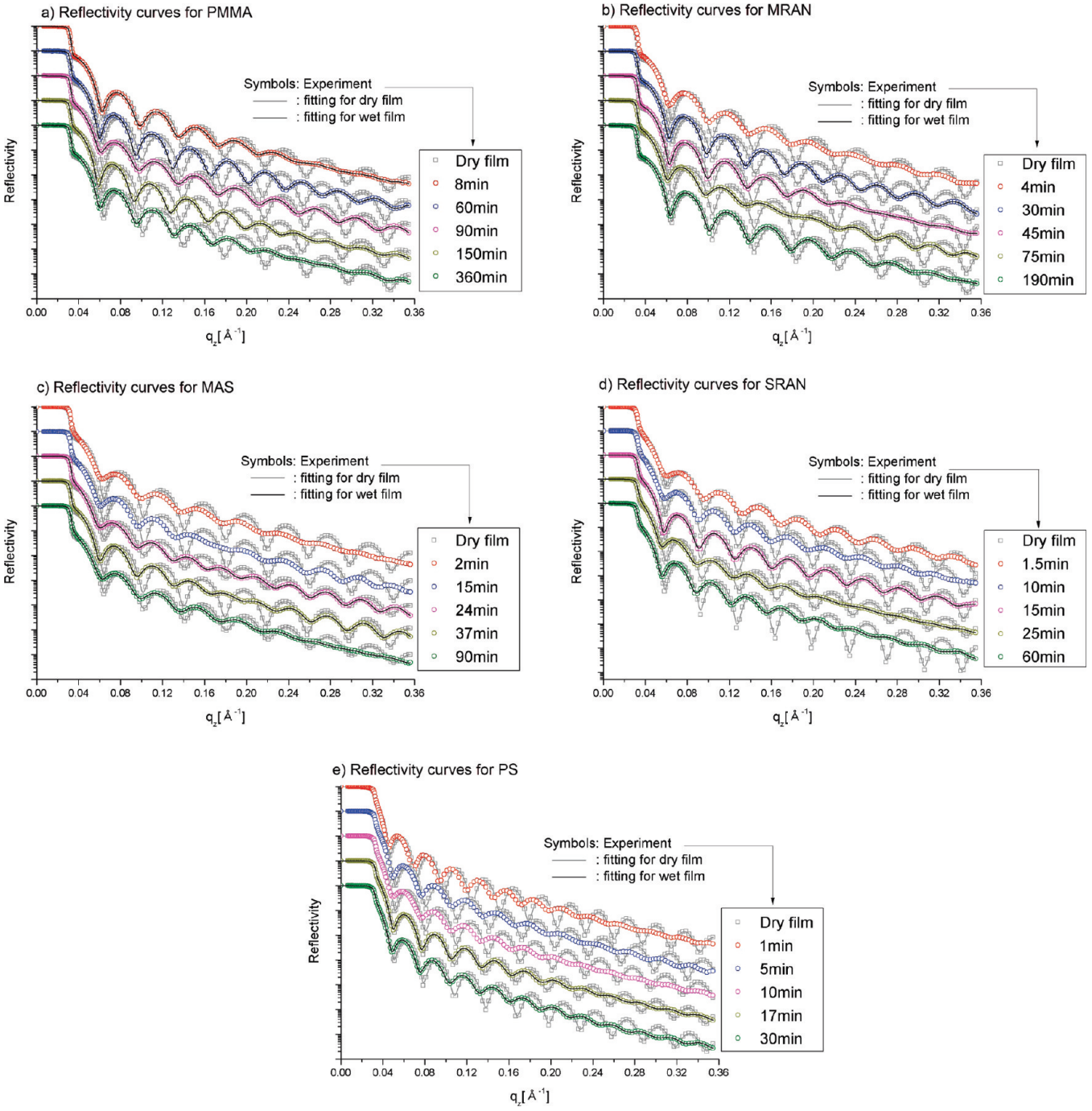

Figure 4. Reflectivity curves for each polymer film. Symbols represent measured values: gray, reflectivity before water contact; color, reflectivity after water contact. Solid lines represent fitting results. For clarity, curves are offset from neighbors by one decade.

that it occurred because of the hydrophilic nature of silicon oxide, without reference to any polymeric effects. However, the polymeric effects cannot be ignored because water molecules diffuse into the free space between the polymer chains. In particular, if the vertical density distribution of a polymer film is assumed to be uniform, then the localization of water within the film−substrate interfacial region makes the vertical density profiles of whole system more irregular than before water contact. The diffusion process suggested in our result is plausible even from the viewpoint of density uniformity because the density uniformity is recovered as the diffusion of water into the film proceeds.

The second group of films includes MAS, SRAN, and PR (Figure 7). The observation that the diffusion behavior in MAS resembles that in PS and not PMMA, even though MAS is 46% PS and 54% PMMA (mol fraction), is consistent with the affinity between density distributions of MAS and PS films described in a previous study.[19] In this group of films, increases in the density distributions following water contact were also observed, which may be due to the accumulation of water inside films. The water seemed to accumulate in low-density regions to recover the uniformity of the density distribution, especially in SRAN and PS. However, the densities in the depletion layer did not increase. We do not know what preserves the density depletion near the polymer/substrate interface even after water

Table 2. Summary of Fitting Results for Five Stages of Water Diffusion in Five Polymer Films[a]

Increasing MMA Portion	Stages of water diffusion: Stage 1	Stage 2	Stage 3	Stage 4	Stage 5
PMMA	1		2	3	3
MRAN				2	3
MAS				4	3, 4
SRAN				3, 4	3, 4
PS					3, 4

[a] White cells indicate that the electron density distributions of the films are obtained normally from fitting process, and gray cells indicate the fitting failure. Codes: (1) The thickness is changed, but the overall changes in film density distribution are insignificant. (2) An abrupt density increase occurred near the interface region after water contact, possibly because of water accumulation. (3) Diffusion is saturated. (4) The density distribution at the film surface is diffused after water contact.

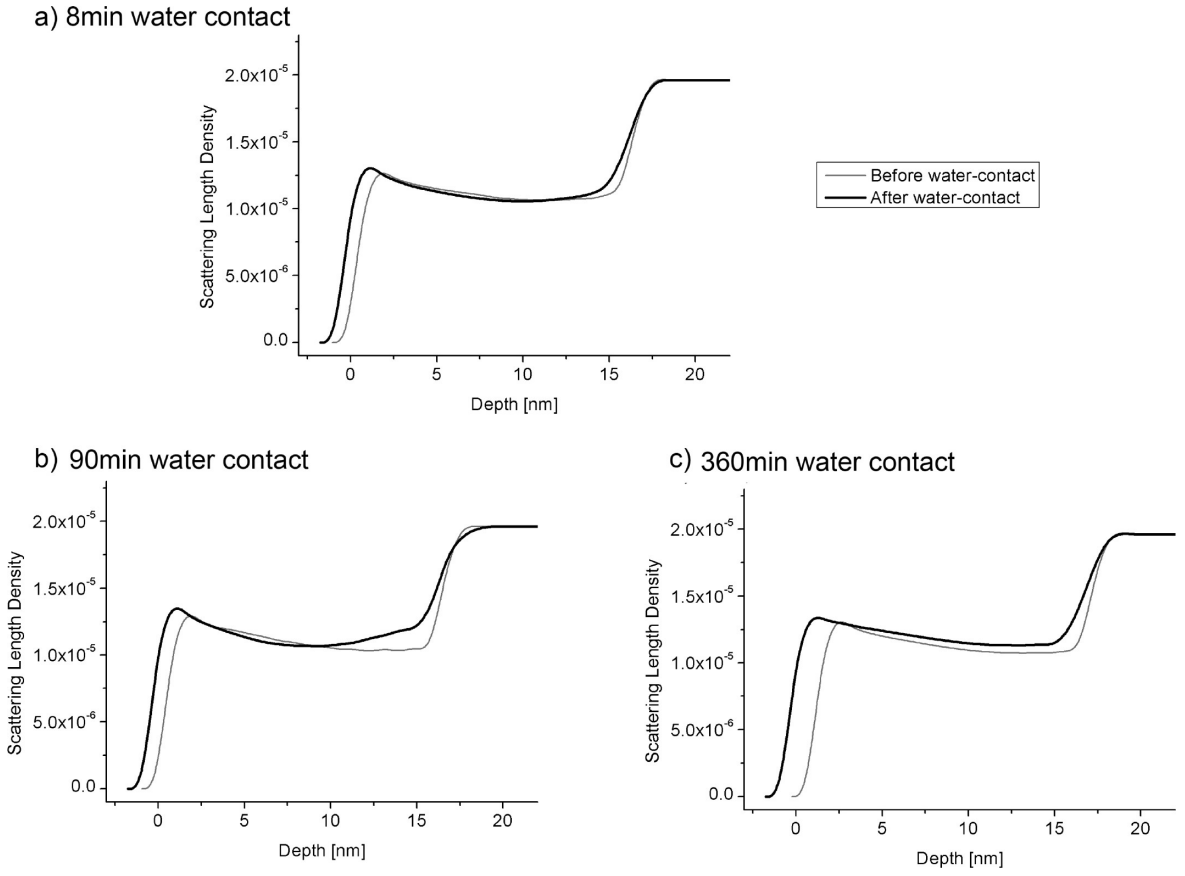

Figure 5. Scattering length density distributions for PMMA films before and after (a) 8 min (stage 1), (b) 90 min (stage 3, i.e., the water-rich interface between the film and substrate), and (c) 360 min (saturated stage of diffusion) of water contact. Gray lines, before water contact; black lines, after water contact. All plots are aligned with the interface between the polymer and the Si substrate. The unit of the scattering length density is $Å^{-2}$, and the calculated scattering length density from the common bulk PMMA density is 1.08×10^{-5} $Å^{-2}$ (cf. 9.1×10^{-6} $Å^{-2}$ for PS).

contact or what physical phenomena occur in this region during water contact. Further studies are required to understand these effects.

The density diffusivities at the surfaces of MAS, SRAN, and PS increased after sufficient water contact (Figure 7). In fact, there is one possibility that the fitting program yields a wrong answer because reflectivity curves of the interface−diffuse film and the surface−diffuse film are similar. To test this possibility, simulations of the reflectivity curves of the interface−diffuse film and the surface−diffuse film were performed: the reflectivity curve of the interface−diffuse film had larger oscillation amplitudes at low angle than did the curve of the surface−diffuse film (Figure 8). The amplitudes of the first oscillations for wet PMMA and MRAN did not noticeably change after water contact, but those for the other films were reduced (Figure 4). These observations indicate that the increase in surface diffusivity for wet films of this group is a real phenomenon. In fact, the roughness of a polymer film

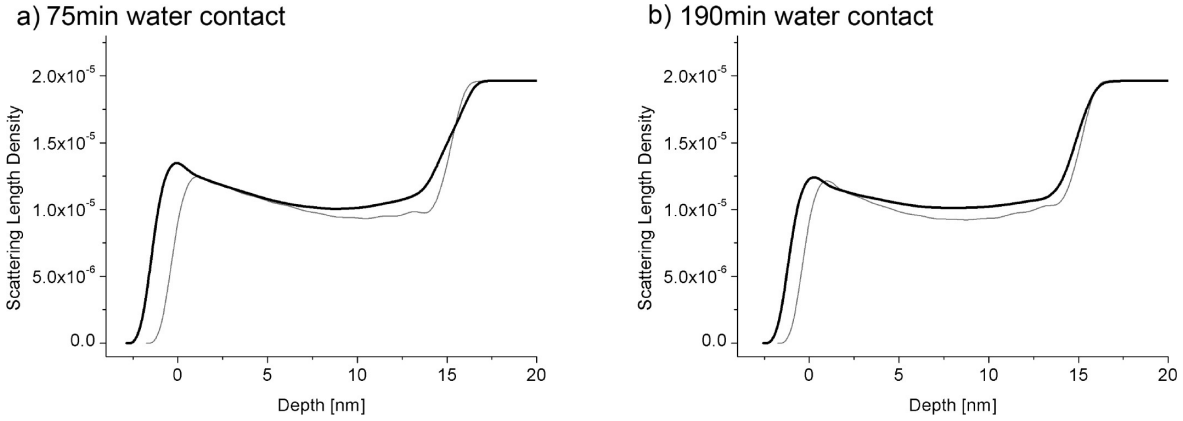

Figure 6. Scattering length density distributions for MRAN (random copolymer with an 88% MMA mol fraction) films before and after (a) 75 min (stage 4, i.e., water-rich interface between the film and substrate) and (b) 190 min (saturated stage of diffusion) of water contact. All plots are aligned with the interface between the polymer and the Si substrate.

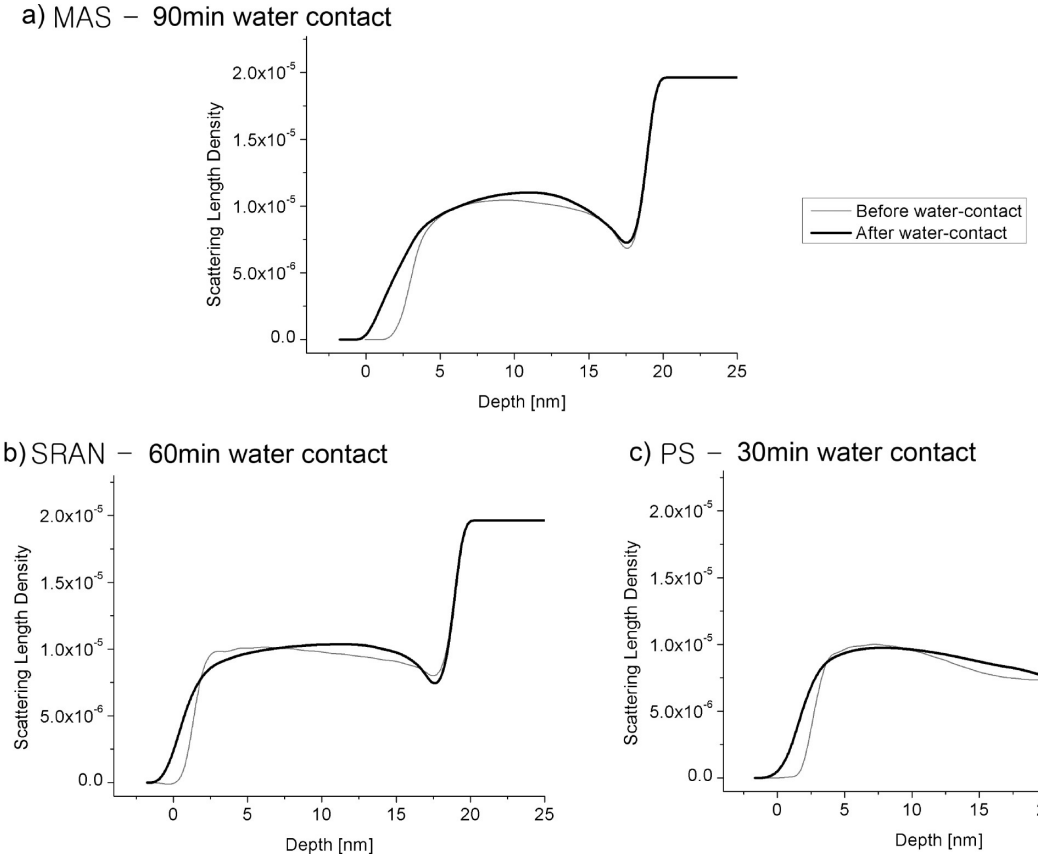

Figure 7. Scattering length density distributions for (a) MAS (a random copolymer with a 54% MMA mol fraction) films before and after 90 min of water contact, (b) SRAN (a random copolymer with a 16% MMA mol fraction) films before and after 60 min of water contact, and (c) PS films before and after 30 min of water contact. Each water contact time corresponds to the saturated final stage of diffusion (stage 5). All plots are aligned with the interface between the polymer and the Si substrate.

increases after direct water contact;[40] this finding is consistent with the XRR results, although the film materials and thicknesses are slightly different. Therefore, AFM analysis was performed on the films in this study to examine the change in roughness after water contact.

3.4. AFM Measurement. In representative AFM images of the two groups of films, the surface roughness of the PMMA film barely changed even after long-term (360 min) water contact (Figure 9a,b). However, in MAS, SRAN, and PS (especially SRAN) films, the surface roughness changed noticeably even after a short period (5 min in the case of the SRAN film) of water contact. Comparisons of SRAN films (Figure 9c–e) disclose that the roughness change after water contact was related to the water contact time and that the morphology of the SRAN sample was affected by direct water contact much more rapidly than was the morphology of the PMMA or MRAN film. The dependency of film roughness on water contact time indicates that the

(40) Ahn, S. I.; Kim, J. H.; Zin, W. C. *J. Appl. Polym. Sci.* **2007**, *104*, 2361–2365.

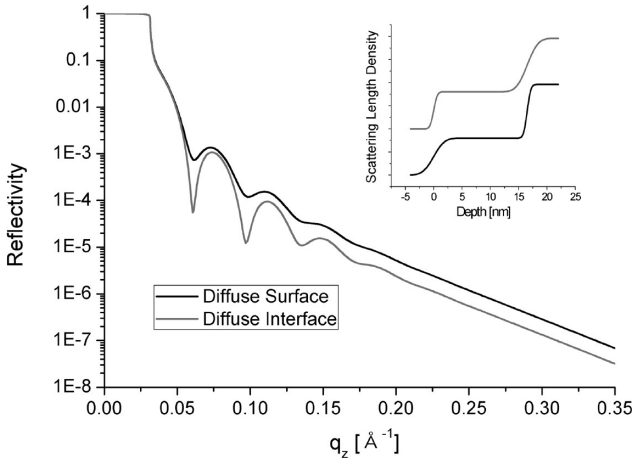

Figure 8. Simulations of the difference between the reflectivity curves from the surface−diffuse film and interface−diffuse film. The inset represents the scattering length density distributions for each simulated film.

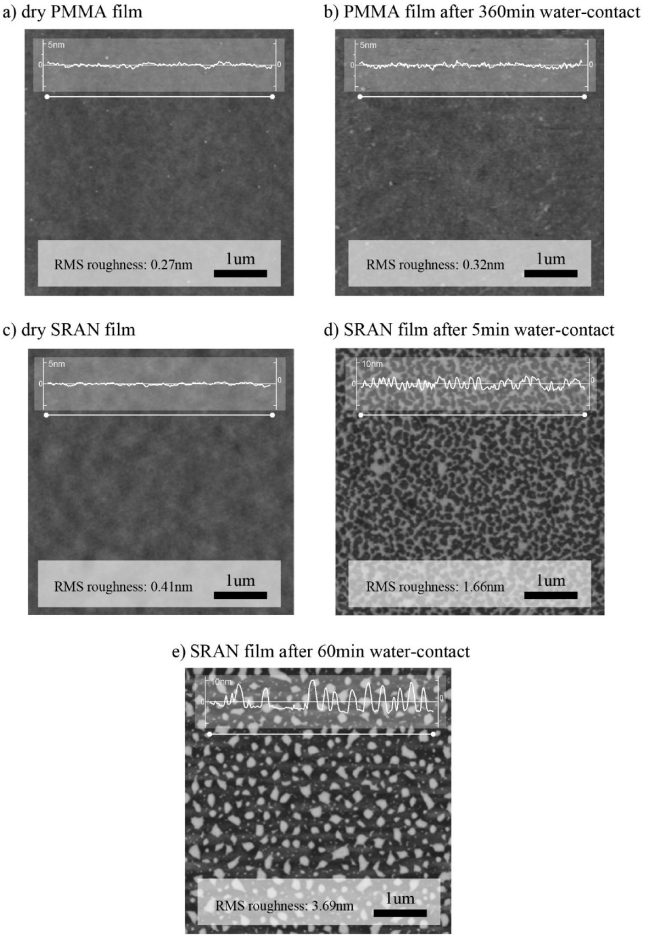

Figure 9. Representative AFM images of PMMA films (a, b) and SRAN films (c−f) before and after water contact. The degree of brightness indicates the height of the film surface. Identical color scales for heights (20 nm) are used for all images.

surfaces of polymer films are directly deformed by water contact.

The mechanism underlying the drastic changes in surface roughness after water contact is unknown; however, surfaces of PS- and styrene-rich films are clearly deformed to a greater degree than PMMA film surfaces even after short water contact times. Thus, the consistent results obtained from the XRR and AFM analyses can be explained by the same possible suggestions. In spite of sufficient annealing at a temperature above T_g, direct water contact on the surface of a polymer film may cause the rearrangement of polymer chains at the water−film interface because the mobility of chains at the surface is higher than that in the bulk.[41−43] In particular, the selective interaction between water molecules and pendant groups in random copolymers can be the reason for the rearrangement of chains. In addition, increasing the styrene content may lead to a greater roughness increase after water contact because water diffuses faster in PS films than in PMMA films as XRR results show in this study.

4. Conclusions

The diffusion behavior of water in films of PMMA/PS homopolymers and random copolymers was investigated using XRR. Two types of diffusion behavior were found in those polymers, which corresponded to the overall shape of the density profiles in the polymers.

At certain stages of diffusion, a density-rich layer, which may correspond to a water-rich layer, was found near the interfacial region of the PMMA and MRAN films. This stage of diffusion was also reported in the literature[10,12] and is regarded as the equilibrium state of diffusion. After prolonged water contact in this study, however, the water molecules spread throughout the films from the interface. The results for density distributions of polymer films in this study commonly present a relatively low density near the film−substrate interface because of the changes in density distributions after water contact in which priority is given to interfacial accumulation in order to obtain the density uniformity of the system.

The initial stages of water diffusion into MAS, SRAN, and PS films could not be observed because the changes in the films occurred over a timescale that was shorter than the measurement time. Instead, a diffusivity of density increase near the surface region was observed; we hypothesized that this enhanced diffusivity may be related to an increase in actual surface roughness during water contact; the increase in surface roughness was confirmed by AFM analysis. Although the water contact time was reduced for these films with high styrene content, the effect of water contact in these films was greater than the effect in PMMA or MRAN films. The greater diffusion coefficient of water in PS and the selective interaction between the water molecules and polymer chains were suggested reasons for this result.

Acknowledgment. We thank Dr. A. van der Lee for providing the fitting program and for many valuable discussions. We also thank Samsung Electronics Co., Ltd. and Dongjin Semichem Co., Ltd. for funding this research. This research was supported by the Basic Science Research Program through the National Research Foundation of Korea (NRF) funded by the Ministry of Education, Science and Technology (2009-0074195).

(41) Forrest, J. A.; DalnokiVeress, K.; Dutcher, J. R. *Phys. Rev. E* **1997**, *56*, 5705–5716.
(42) Frank, B.; Gast, A. P.; Russell, T. P.; Brown, H. R.; Hawker, C. *Macromolecules* **1996**, *29*, 6531–6534.
(43) Kim, J. H.; Jang, J.; Zin, W. C. *Langmuir* **2001**, *17*, 2703–2710.